



Modal interactions in resonant metamaterial slabs with losses

G. Lovat^{a,*}, P. Burghignoli^{b,1}, A.B. Yakovlev^{c,2}, G.W. Hanson^{d,3}

^a Department of Electrical Engineering, “Sapienza” University of Rome, Via Eudossiana 18, 00184 Rome, Italy

^b Department of Electronic Engineering, “Sapienza” University of Rome, Via Eudossiana 18, 00184 Rome, Italy

^c Department of Electrical Engineering, University of Mississippi, University, MS 38677-1848, USA

^d Department of Electrical Engineering and Computer Science, University of Wisconsin-Milwaukee, 3200 N. Cramer St., Milwaukee, WI 53211, USA

Received 13 July 2008; received in revised form 19 September 2008; accepted 22 September 2008

Abstract

Modal phenomena in planar metamaterial structures modeled by simple scalar frequency-dependent constitutive parameters are investigated. Modal interactions and modal transformations are found in frequency ranges close to the medium resonances when material losses are introduced and their level is continuously varied through certain critical values. Numerical results for TE and TM modes of a grounded metamaterial slab are reported in the form of dispersion curves and pole loci in the complex wavenumber plane for both surface- and leaky-wave propagation regimes. Useful insights into the reported results are provided through the identification of the branch-point singularities in the complex frequency plane that govern the modal interactions.

© 2008 Elsevier B.V. All rights reserved.

PACS: 41.20.Jb (electromagnetic wave propagation, radiowave propagation)

Keywords: Metamaterial slab; Modal interaction; Surface waves; Leaky waves; Resonant media; Planar waveguides

1. Introduction and background

Electromagnetic features of metamaterial slab waveguides have been the subject of many investigations in the last decade, in view of their potential use as constituent parts (e.g., substrates) of microwave guiding and radiating devices. Considering in particular the propagation of surface (*bound*) and leaky (*radiating*) modes,

various peculiar properties have been pointed out, e.g., the transverse field configuration of the modes, energy propagation in backward surface waves, surface-wave suppression in grounded slabs, unimodal propagation in non-radiative dielectric waveguides derived thereof, and backward radiation from proper leaky waves (see, e.g., [1–9]).

Although artificially engineered materials can be anisotropic (and possibly also spatially dispersive, as in the case of the wire medium and other complex media, see, e.g., [10,11]), homogenized isotropic lossless models have often been assumed in the above-mentioned investigations, with frequency-dispersive material parameters obeying Lorentz-like dispersion laws for the permeability and Drude-like laws for the permittivity. In any case, a typical feature of such models is the existence of *resonances* in the electromagnetic

* Corresponding author. Fax: +39 06 4742647.

E-mail addresses: giampiero.lovat@uniroma1.it (G. Lovat), burghignoli@die.uniroma1.it (P. Burghignoli), yakovlev@olemiss.edu (A.B. Yakovlev), george@uwm.edu (G.W. Hanson).

¹ Fax: +39 06 4742647.

² Fax: +1 662 915 7231.

³ Fax: +1 414 229 6958.

response of the material, i.e., frequencies for which the material parameters tend to infinity.

This paper proposes a first systematic study of the effects of realistic material losses on the dispersion properties of modes supported by a grounded isotropic metamaterial slab. In particular, the study is focused on a frequency region close to a permeability resonance, in which, by increasing frequency and in the absence of losses, the material changes from Epsilon Negative (ENG) to Double Negative (DNG). The addition of magnetic losses to the metamaterial model will be shown to result in interesting evolutions and interactions of different modal solutions, as already reported for slab waveguides made of different ordinary materials [12–16]. Both TE and TM modes are considered, showing how, as for ordinary slabs, their interactions can be interpreted in terms of suitable complex frequency-plane branch points. Some preliminary results have been presented in a recent conference [17].

The paper is organized as follows. In Section 2, the basic concepts and dispersion equations of the Drude/Lorentz homogenization model of metamaterial slab are described. Dispersion properties of TE and TM natural modes of metamaterial slab in the absence of losses are illustrated in Section 3. Section 4 focuses on the analysis and explanation of modal interactions in the presence of magnetic loss. In Section 5 some concluding remarks are given.

2. Resonant metamaterial model

The slab waveguide considered here consists of a grounded slab of thickness h (see the inset of Fig. 1(a)) made of a homogeneous and isotropic metamaterial with constitutive parameters described by a Lorentz dispersion law for the permeability and a Drude law for the permittivity:

$$\mu_r(\omega) = 1 - \frac{\omega_{mp}^2 - \omega_0^2}{\omega^2 - \omega_0^2 - j\gamma_m\omega} \quad (1)$$

$$\epsilon_r(\omega) = 1 - \frac{\omega_{ep}^2}{\omega^2 - j\gamma_e\omega}$$

In (1), the parameters γ_m and γ_e account for magnetic and electric losses, respectively. In the numerical simulations the following values for the parameters in (1) have been assumed: $\omega_0/2\pi = 21$ GHz, $\omega_{mp}/2\pi = 24.5$ GHz, $\omega_{ep}/2\pi = 28$ GHz, and $\gamma_e = 0$ GHz (i.e., no electric losses) [18]. It should be noted that the effects of modal interactions presented in this paper have also been found in other classes of resonant metamaterials, such as resonant-sphere media [19]. The qualitative behavior of

the modes discussed in this work should hold generally for metamaterials that can be suitably homogenized (i.e., modeled as a continuum medium that is isotropic and local) at frequencies where the homogenized permittivity is smoothly varying and the homogenized permeability undergoes a resonance.

The dispersion equations for the isotropic metamaterial slab are the same as for an ordinary slab [6],

$$Z^{TE}(k_t) = j \frac{\omega\mu_0\mu_r}{k_{ys}} \tan(k_{ys}h) + \frac{\omega\mu_0}{k_{y0}} = 0 \quad (2)$$

$$Z^{TM}(k_t) = j \frac{k_{ys}}{\omega\epsilon_0\epsilon_r} \tan(k_{ys}h) + \frac{k_{y0}}{\omega\epsilon_0} = 0 \quad (3)$$

where $k_{y0} = \sqrt{k_0^2 - k_t^2}$, $k_{ys} = \sqrt{k_s^2 - k_t^2}$, $k_0^2 = \omega^2\mu_0\epsilon_0$, $k_s^2 = k_0^2\mu_r\epsilon_r$, and k_t is the unknown propagation wavenumber. Note that ϵ_r and μ_r are frequency-dispersive relative permittivity and permeability described by (1).

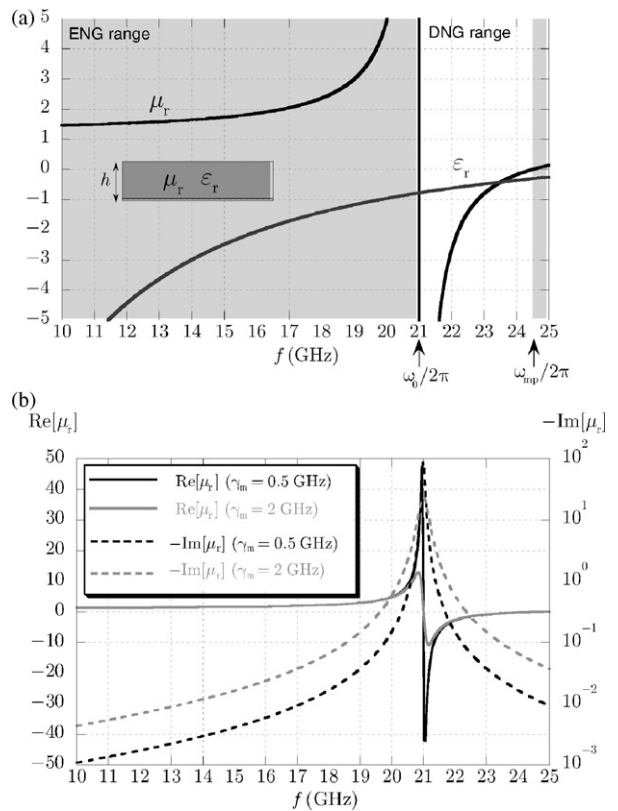


Fig. 1. (a) Relative permeability and permittivity of the grounded metamaterial slab considered here (shown in the inset) as a function of frequency, in the absence of losses. (b) Real and imaginary parts of the relative magnetic permeability for two values of the magnetic-loss parameter γ_m . Parameters of the Lorentz–Drude models: $\omega_0/2\pi = 21$ GHz, $\omega_{mp}/2\pi = 24.5$ GHz, and $\omega_{ep}/2\pi = 28$ GHz.

In Fig. 1(a) the relative permittivity and permeability are shown as a function of frequency for a lossless structure in a wide frequency range, including two ENG ranges ($f < f_0 = \omega_0/2\pi = 21$ GHz and $f > f_{mp} = \omega_{mp}/2\pi = 24.5$ GHz, shaded areas) and one DNG range (between f_0 and f_{mp} , transparent area). The vertical asymptote of the relative permeability is clearly visible at $f = f_0 = 21$ GHz (magnetic resonance).

In Fig. 1(b), the real part of the relative permeability and the magnetic loss tangent are shown for two lossy cases, with $\gamma_m = 0.5$ GHz and $\gamma_m = 2$ GHz, respectively. When losses are introduced in the dispersive model, the relative permeability has a real part that remains finite at $f = f_0$ and a nonzero imaginary part, having peak close to f_0 .

3. Modal solutions in the absence of losses

In this section we study the dispersion behavior of TE and TM modes of the lossless metamaterial slab and the pole dynamics of complex solutions transitioning from the DNG region to the ENG region across the magnetic resonance of 21 GHz. Although the dispersion curves of such a structure have already been studied in [6] in the absence of losses, the analysis presented here will be helpful for understanding of modal behavior in the presence of magnetic loss, which is described in the section to follow.

In Fig. 2(a) and (b) dispersion curves are reported for the normalized phase (β/k_0) and attenuation (α/k_0) constants of two TE modes (labeled here TE₂ and TE₃ according to [6]) of a grounded metamaterial slab with parameters as in (1) and thickness $h = 5$ mm. (Here and in the following solid lines are used to indicate proper modes, whereas dashed lines are used to label improper modes.) In Fig. 2(c) the corresponding curves in the complex plane of the normalized wavenumber $k_t = \beta - j\alpha$ are shown. In the lossless case, for a given wavenumber k_t that satisfies the dispersion equations, $-k_t$, the conjugate of k_t , and the conjugate of $-k_t$ are also solutions [20]; however, only two of the four wavenumbers associated with each mode are reported for clarity. It can be observed that, at the resonant frequency $f_0 = 21$ GHz, at which the relative permeability tends to infinity, all modal wavenumbers tend to complex infinity. In particular, approaching f_0 from below (i.e., from the ENG range), the modes are improper complex and their attenuation constant tends to infinity while their phase constant tends to zero, hence their wavenumber approaches the imaginary axis. Approaching 21 GHz from above (i.e., from the DNG range), the modes are real and their wavenumber tends to infinity along the real axis. Note

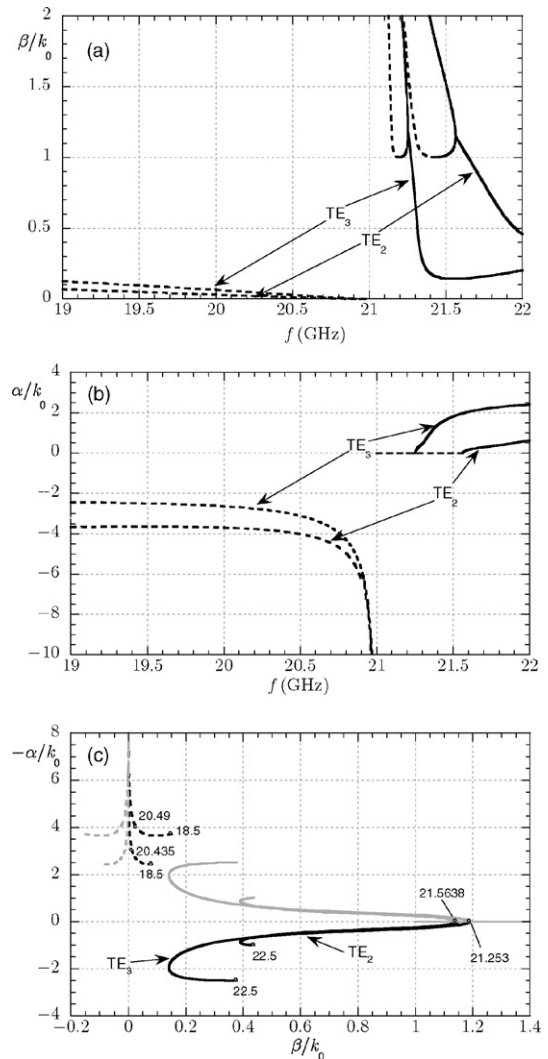


Fig. 2. Dispersion diagrams for the TE₂ and TE₃ modes on a grounded slab with material parameters as in Fig. 1 and thickness $h = 5$ mm, in the absence of losses: (a) normalized phase constant; (b) normalized attenuation constant; (c) evolution in the complex plane of two of the four wavenumbers associated with each mode. Legend: solid lines, proper modes; dashed lines, improper modes.

that, in this lossless case, the real TE₂ and TE₃ modes become complex proper by increasing frequency in the DNG range, and above $f_{mp} = 24.5$ GHz they change again from complex proper to complex improper [5] (not shown in Fig. 2). The splitting-point frequencies above the magnetic resonance at 21 GHz are explicitly indicated in Fig. 2(c) (they are 21.253 GHz for the TE₃ mode and 21.5638 GHz for the TE₂ mode): At these points, representing a proper complex cutoff, modes and their conjugates meet. As described in [12,13], the splitting-point frequency represents a complex frequency-plane

branch point, defined by the conditions [12–14]

$$Z(k_t, \omega) = \frac{\partial Z(k_t, \omega)}{\partial k_t} = 0 \quad (4)$$

$$\frac{\partial Z(k_t, \omega)}{\partial \omega} \frac{\partial^2 Z(k_t, \omega)}{\partial k_t^2} \neq 0 \quad (5)$$

where $Z = Z^{\text{TE}}$ or $Z = Z^{\text{TM}}$ (see Eqs. (2) and (3)) for TE and TM modes, respectively. This branch point is associated with the relatively simple case of connecting a mode and its conjugate. Complex frequency-plane branch points that connect different modes within a given

class (TE or TM) are described later. The behavior of TM modes in the lossless case is illustrated in Fig. 3 for a pair of modes labeled TM_2 and TM_3 (according to terminology used in [6]). The pole evolution in the complex plane is quite similar to that of the TE poles; in this case, however, the complex proper modes remain complex proper, and do not become complex improper (as the TE modes do), both in the ENG and DNG ranges [5].

In the next section the effect of magnetic losses is explored in the critical frequency region close to f_0 , where the lossless metamaterial changes from ENG to DNG.

4. Modal interactions in the presence of magnetic losses

In this section, the evolution of dispersion behavior and pole dynamics of TE and TM modes with varying magnetic loss is studied, leading to the explanation of modal interactions for critical values of loss in terms of complex frequency-plane branch-point singularities.

4.1. TE modes

Fig. 4 shows pole loci obtained from Fig. 2(c) when perturbed by the addition of magnetic loss. Note that in this case modal symmetry is broken, and modes and their conjugates no longer simultaneously satisfy the dispersion equations, although modes and their negatives continue to do so [20]. In Fig. 4(a) the results are shown for the case of $\gamma_m = 0.5$ GHz; the most evident difference with respect to the lossless case is that poles do not tend to complex infinity when f approaches f_0 , rather they move along large loops (in the first quadrant for the poles depicted in the figure) when the frequency varies in a small neighbourhood of f_0 . By increasing the level of magnetic losses to $\gamma_m = 2$ GHz, those loops tend to shrink, as shown in Fig. 4(b); however, a further and more interesting effect takes place: by comparing Fig. 4(a) and (b) a qualitatively different behavior of the curves may be observed in the fourth quadrant. This is made clearer in Fig. 5, where enlarged versions of the same pole loci are reported (see Fig. 5(a) and (b), respectively).

To illustrate the process through which the above-mentioned qualitative change takes place, the evolution of poles in the fourth quadrant is represented in Fig. 6 for different values of γ_m , starting from the lossless case of $\gamma_m = 0$ GHz as shown in Fig. 6(a). The mode identity is still recognizable in Fig. 6(b), corresponding to $\gamma_m = 0.5$ GHz; however, this is not the case in Fig. 6(c), when $\gamma_m = 2$ GHz. By considering in detail the pole evo-

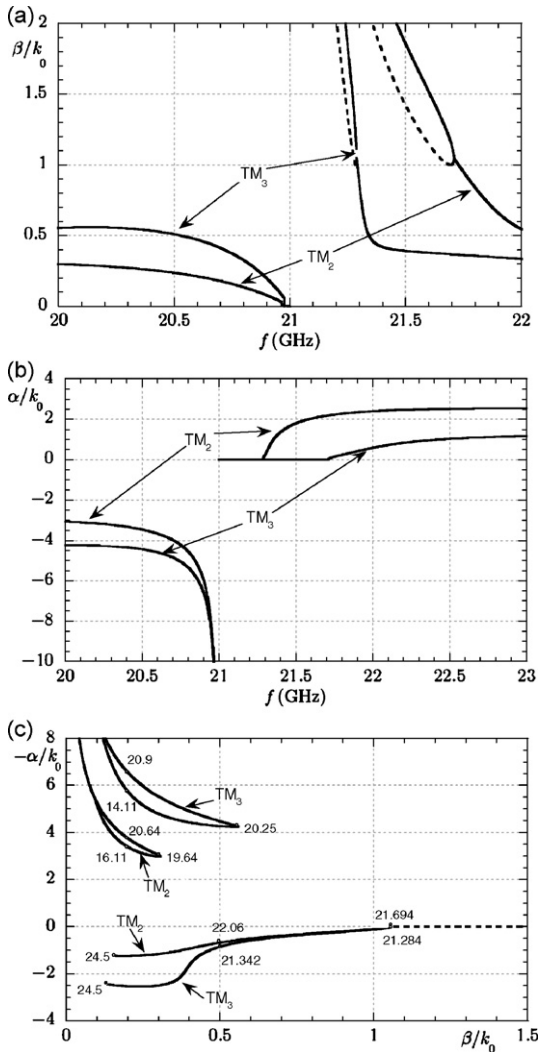


Fig. 3. Dispersion diagrams for the TM_2 and TM_3 modes on a grounded slab with material parameters as in Fig. 1 and thickness $h = 5$ mm, in the absence of losses: (a) normalized phase constant; (b) normalized attenuation constant; (c) evolution in the complex plane of one of the four wavenumbers associated with each mode. Legend: as in Fig. 2.

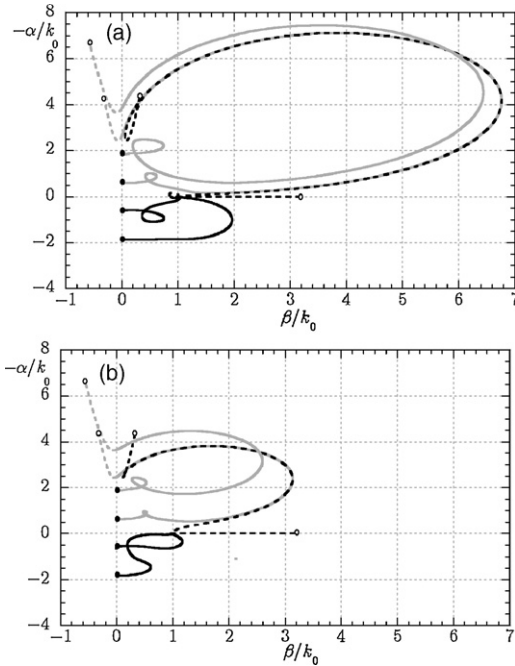


Fig. 4. Evolution in the complex plane of two of the four wavenumbers associated with each of the TE₂ and TE₃ modes in the presence of magnetic losses, obtained starting from high frequencies. (a) $\gamma_m = 0.5$ GHz; (b) $\gamma_m = 2$ GHz. The closed circles indicate the points corresponding to $f = 24.5$ GHz, while the open circles indicate the points corresponding to $f = 10$ GHz. Legend: as in Fig. 2.

lution for values of γ_m in between, it has been found that a sudden qualitative change occurs at a specific, critical value of the loss parameter, $\gamma_{mcr} = 0.975638$ GHz; this is illustrated in Fig. 6(d), where pole loci are shown for values of immediately below, equal to, and immediately above γ_{mcr} : a typical mode interaction is observed, in which the perturbed TE₂ and TE₃ modes exchange their character; exactly at $\gamma_m = \gamma_{mcr}$ the two perturbed curves simply intersect.

The modal interaction can be interpreted by studying the evolution of the complex frequency-plane branch point that connects the TE₂ and TE₃ modes. As described in [12,14], various types of branch points occur in the complex frequency plane that govern the modal behavior in the complex wavenumber plane. In particular, two types of branch points are relevant here. As previously described, when a mode meets its complex conjugate this indicates a first-order branch point, $\omega = \omega^{(1)}$. Furthermore, when two different modes within a mode class (TE or TM) meet, this indicates a different type of complex frequency-plane branch point, $\omega = \omega^{(2)}$ [12–14], which satisfies the same conditions as $\omega^{(1)}$, (4) and (5). Here, a branch point of $\omega^{(2)}$ -type was found to occur for $\gamma_m = \gamma_{mcr}$ on the real frequency axis

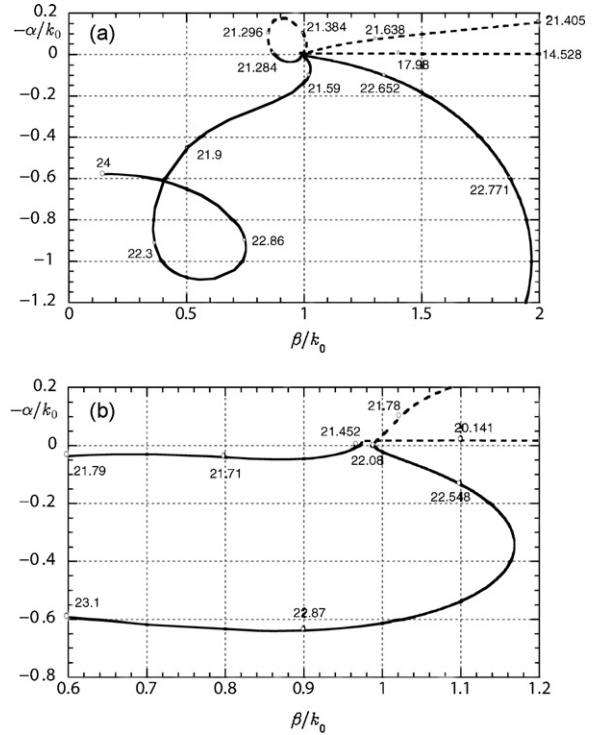


Fig. 5. (a) Enlarged plot of Fig. 4(a) (case $\gamma_m = 0.5$ GHz); (b) enlarged plot of Fig. 4(b) (case $\gamma_m = 2$ GHz).

at $f_{cr} = 22.8237419$ GHz, and in the complex wavenumber plane at $\beta_{cr}/k_0 = 1.0009997$ and $\alpha_{cr}/k_0 = 1.1378933$. More generally, the evolution of the branch point in the complex frequency plane as a function of the magnetic-loss parameter γ_m in the range from 0 to 2 GHz is shown in Fig. 7. For $\gamma_m < \gamma_{mcr}$ the branch point is in the lower-half frequency plane, and for $\gamma_m > \gamma_{mcr}$ the branch point is in the upper-half plane, crossing the real frequency axis at $\gamma_m = \gamma_{mcr}$. As frequency is varied (implicitly, along the real axis), the branch point is passed on different sides for $\gamma_m < \gamma_{mcr}$ and $\gamma_m > \gamma_{mcr}$. Since in encircling the branch point the TE₂ and TE₃ modes become interchanged, the interpretation assigned to a given solution of the dispersion equation depends on the path of frequency variation, and on the location of the branch point relative to that path [12,14]. For $f = f_{cr}$ the curves intersect, as shown in Fig. 6(d). Thus, the mode interaction and mode transformation can be understood in the context of the branch point that governs a particular mode pair.

4.2. TM modes

The effect of introducing losses on the TM pole evolution is illustrated in Fig. 8 with reference to the TM₂

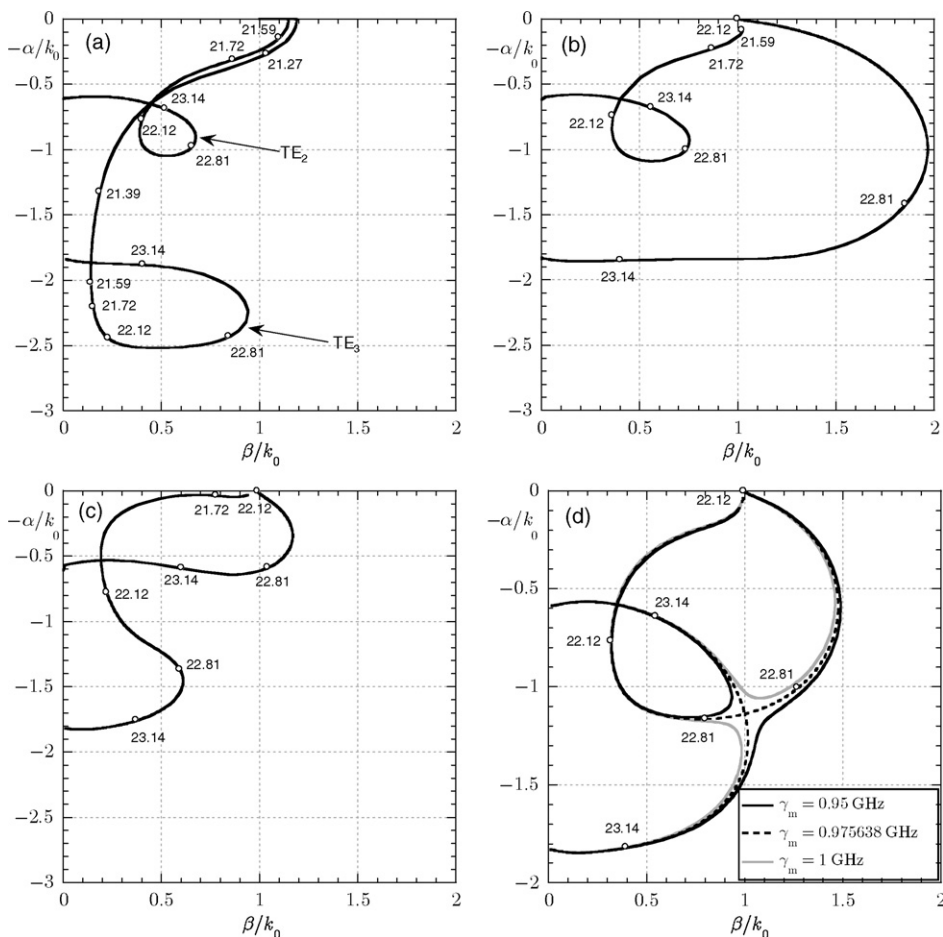


Fig. 6. Evolution in the fourth quadrant of the complex plane of wavenumbers associated with the TE₂ and TE₃ modes: (a) lossless case ($\gamma_m = 0$ GHz); (b) $\gamma_m = 0.5$ GHz; (c) $\gamma_m = 2$ GHz; (d) critical value $\gamma_m = 0.975638$ GHz.

and TM₃ modes shown in Fig. 3 in the lossless case. In particular, we focus our attention on the TM₂ pole in the fourth quadrant (*black line*). By decreasing frequency, that pole migrates in the fourth quadrant until it crosses the Sommerfeld branch cut on the positive real axis. Then it enters the first quadrant of the improper Riemann sheet, where it moves along a loop in a narrow frequency range; finally, it crosses the branch cut again on the positive imaginary axis and enters the second proper quadrant.

In Fig. 8(a) and (b) it can be observed that, by increasing the level of magnetic losses, the point where a pole locus intersects the branch cut on the positive real axis shifts towards the origin of the complex plane. Of course, the same happens for the pole located symmetrically with respect to the origin in the second quadrant (*gray line*). Above a certain level of losses,

the qualitative behavior of the pole locus changes, as it can be seen in Fig. 8(c); by decreasing frequency, the TM₂ pole enters the third (improper) quadrant rather than the first. The critical value of γ_m for which the change takes place is $\gamma_{mcr} = 2.4439924$ GHz as illustrated in Fig. 9; when $\gamma_m = \gamma_{mcr}$ the crossing of the branch cut occurs exactly at the origin of the complex plane.

As in the TE case, the above-described TM modal interaction can be explained in terms of a suitable frequency-plane singularity. In particular, a frequency-plane branch point can be found that crosses the real axis in the complex frequency plane when $\gamma_m = \gamma_{mcr}$ and thus determines a qualitative change in the shape of the pole loci and of the relevant dispersion diagrams (the latter are reported in Fig. 10 for the cases in Fig. 8).

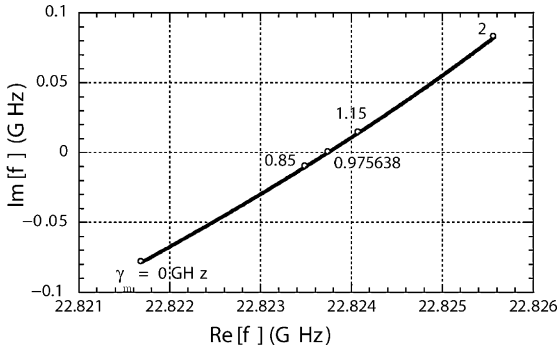


Fig. 7. Evolution of the branch-point singularity in the complex frequency plane associated with the TE_2/TE_3 modal interaction, as a function of the magnetic-loss parameter γ_m in the range from $\gamma_m=0$ GHz to $\gamma_m=2$ GHz.

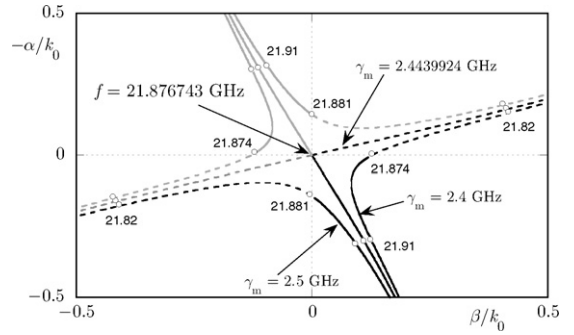


Fig. 9. Evolution in the complex plane of wavenumbers associated with the TM_2 mode: three lossy cases, including the critical value $\gamma_m=2.4439924$ GHz.

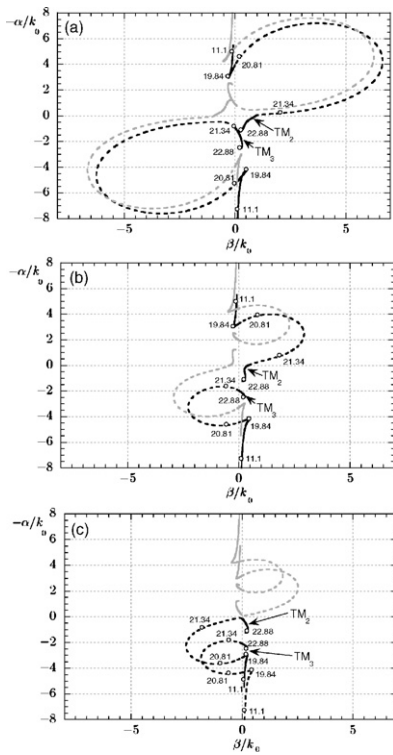


Fig. 8. Evolution in the complex plane of two of the four wavenumbers associated with each of the TM_2 and TM_3 modes in the presence of magnetic losses, obtained starting from high frequencies: (a) $\gamma_m=0.5$ GHz; (b) $\gamma_m=2$ GHz; (c) $\gamma_m=2.5$ GHz.

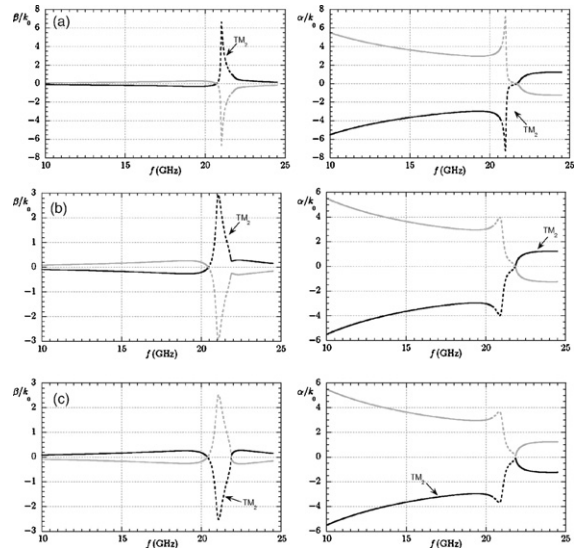


Fig. 10. Dispersion diagrams for the TM_2 mode in the presence of magnetic losses, corresponding to the cases in Fig. 8: (a) $\gamma_m=0.5$ GHz; (b) $\gamma_m=2$ GHz; (c) $\gamma_m=2.5$ GHz.

5. Conclusion

Modal behavior on a grounded, isotropic metamaterial slab have has been described in the presence of magnetic loss. Modal interactions and modal transformations were found in frequency ranges close to the medium resonances, and the addition of magnetic loss has been shown to qualitatively change the dispersion behavior in these regions. These phenomena have been described in terms of complex frequency-plane branch points that connect various solutions of the dispersion equation (i.e., modes and their conjugates, and different modes in a mode class). This method provides a way to understand complicated modal behavior in a systematic manner.

References

- [1] I.W. Shadrivov, A.A. Sukhorukov, Y.S. Kivshar, Guided modes in negative-refractive-index waveguides, *Phys. Rev. E* 67 (2003) 57602.
- [2] B.I. Wu, T.M. Grzegorzczuk, Y. Zhang, J.A. Kong, Guided modes with imaginary transverse wavenumber in a slab waveguide with negative permittivity and permeability, *J. Appl. Phys.* 93 (2003) 9386–9388.
- [3] I.S. Nefedov, S.A. Tretyakov, Waveguide containing a backward-wave slab, *Radio Sci.* 38 (2003), doi:10.1029/2003RS002900.
- [4] A. Alù, N. Engheta, Guided modes in a waveguide filled with a pair of single-negative (SNG), double-negative (DNG), and/or double-positive (DPS) layers, *IEEE Trans. Microw. Theory Tech.* 52 (2004) 199–210.
- [5] P. Baccarelli, P. Burghignoli, F. Frezza, A. Galli, P. Lampariello, G. Lovat, S. Paulotto, Effects of leaky-wave propagation in metamaterial grounded slabs excited by a dipole source, *IEEE Trans. Microw. Theory Tech.* 53 (2005) 32–44.
- [6] P. Baccarelli, P. Burghignoli, F. Frezza, A. Galli, P. Lampariello, G. Lovat, S. Paulotto, Fundamental modal properties of surface waves on metamaterial grounded slabs, *IEEE Trans. Microw. Theory Tech.* 53 (2005) 1431–1442.
- [7] I. Shadrivov, R. Ziolkowski, A. Zharov, Y. Kivshar, Excitation of guided waves in layered structures with negative refraction, *Opt. Express* 13 (2005) 481–492.
- [8] A.L. Topa, C.R. Paiva, A.M. Barbosa, Novel propagation features of double negative H-guides and H-guide couplers, *Microw. Opt. Technol. Lett.* 47 (2005) 185–190.
- [9] P. Baccarelli, P. Burghignoli, F. Frezza, A. Galli, P. Lampariello, S. Paulotto, Unimodal surface-wave propagation in metamaterial nonradiative dielectric waveguides, *Microw. Opt. Technol. Lett.* 48 (2006) 2557–2560.
- [10] P.A. Belov, R. Marquès, S.I. Maslovski, I.S. Nefedov, M. Silveirinha, C.R. Simovski, S.A. Tretyakov, Strong spatial dispersion in wire media in the very large wavelength limit, *Phys. Rev. B* 67 (2003) 113103.
- [11] C.R. Simovski, Analytical modelling of double-negative composites. *Metamaterials* 2, in press.
- [12] G.W. Hanson, A.B. Yakovlev, Investigation of mode interaction on planar dielectric waveguides with loss and gain, *Radio Sci.* 34 (1999) 1349–1359.
- [13] G.W. Hanson, A.B. Yakovlev, J. Hao, Leaky-wave analysis of transient fields due to sources in planarly layered media, *IEEE Trans. Antennas Propagat.* 51 (2003) 146–159.
- [14] A.B. Yakovlev, G.W. Hanson, Mode-transformation and mode-continuation regimes on waveguiding structures, *IEEE Trans. Microw. Theory Tech.* 48 (2000) 67–75.
- [15] A.B. Yakovlev, G.W. Hanson, Fundamental wave phenomena on biased-ferrite planar slab waveguides in connection with singularity theory, *IEEE Trans. Microw. Theory Tech.* 51 (2003) 583–587.
- [16] A.B. Yakovlev, G.W. Hanson, Fundamental modal phenomena on isotropic and anisotropic planar slab dielectric waveguides, *IEEE Trans. Antennas Propagat.* 51 (2003) 888–897.
- [17] H.A. Olanigan, A.B. Yakovlev, G. Lovat, P. Burghignoli, G.W. Hanson, Modal characterization of lossy metamaterial slab waveguides, in: 2nd European Conference on Antennas and Propagation, Edinburgh, UK, 11–16 November, 2007, pp. 1–6.
- [18] M. Mojahedi, K.J. Malloy, G.V. Eleftheriades, J. Woodley, R.Y. Chiao, Abnormal wave propagation in passive media, *IEEE J. Select. Top. Quantum Electron.* 9 (2003) 30–39.
- [19] A.B. Yakovlev, G. Lovat, P. Burghignoli, G.W. Hanson, Modal interactions in lossy dielectric metamaterial slabs, in: Proceedings of the 2008 USNC/URSI National Radio Science Meeting, San Diego, CA, 5–12 July, 2008.
- [20] J.A. Kong, *Electromagnetic Wave Theory*, Wiley, New York, 1990.